



ELSEVIER

Catalysis Today 46 (1998) 223–231



Oxidative pyrolysis of natural gas in a spouted-bed reactor: reaction stoichiometry and experimental reactor design

G.A. Huff^{*}, I.A. Vasalos¹

Amoco Petroleum Products, PO Box 3011, Naperville, IL 60563, USA

Abstract

A simple reaction network is developed to understand methane oxidative pyrolysis in a spouted-bed reactor. Oxidative pyrolysis for converting natural gas is attractive because it gives high methane conversions (80–90% per pass) at high selectivities to C_{2+} (40%) and carbon monoxide (40%). Based on results reported in a British Petroleum patent, our analysis shows that oxidative pyrolysis is a combination of methane partial oxidation to carbon monoxide which produces heat and of methane pyrolysis to C_{2+} (mostly ethylene and acetylene) which consumes heat. The methane pyrolysis reaction is thermodynamically limited and requires temperatures above 1000°C for significant conversion.

A pilot-plant oxidative pyrolysis reactor was designed from cold flow studies to verify the BP results obtained at atmospheric pressure and to establish process feasibility at higher pressures. Scoping economic studies show that higher pressure operation is needed to avoid costly product compression in downstream upgrading processes. The pilot-plant spouted-bed reactor evolved from a fragile quartz tube to a more robust one of stainless steel. The stainless steel performs similarly to the quartz reactor when the walls are coated with an aluminum oxide layer to passivate inherent catalytic activity. Although a number of experimental challenges remain, initial runs have been successful in demonstrating that our method of preheating the feed successfully ignites the reaction and that our analytical technique gives excellent closure in detailed material balances.

Based on results presented in this paper ways are needed to improve on BP C_{2+} yields, such as by process variable optimization and rapid thermal quench to minimize undesirable secondary pyrolysis reactions. © 1998 Elsevier Science B.V. All rights reserved.

Keywords: Natural gas; Oxidative pyrolysis; Partial oxidation; Ethylene; Acetylene; Olefins; Synthesis gas; Reaction engineering; Methane; Pyrolysis

1. Introduction

Acetylene is known to be produced by the BASF process [1] via partial combustion of natural gas in a special burner at a temperature of about 1300°C and at

a very short reaction time in order to preserve the acetylene formed in the cracking process. The amount of energy required to convert methane to acetylene is provided by the partial combustion of methane. The acetylene formed during the reaction is preserved with quench of the products with large amounts of water.

British Petroleum in [2] and European Patent application 016 486 claim a process for producing synthesis gas and light hydrocarbons by partial oxidation of

^{*}Corresponding author.

¹Present address: CPERI and University of Thessaloniki, PO Box 361, Thessaloniki, 57001 Thessaloniki, Greece.

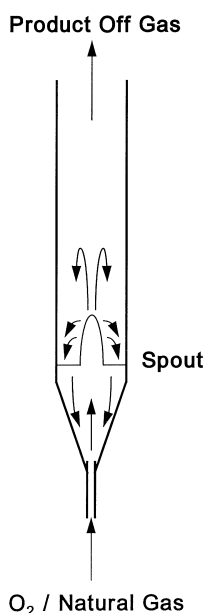


Fig. 1. Spouted-bed reactor for methane oxidative pyrolysis.

methane in a spouted-bed reactor. Methane and oxygen are fed upward through a bed of fine sand particles at a sufficiently high gas velocity to cause a spouting action (see Fig. 1). The methane to oxygen feed ratio is 1.6:1, and adiabatic reaction temperatures reach more than 1090°C. Oxidative pyrolysis is reported to be non-catalytic and self-sustaining once the methane and oxygen are ignited.

The BP work was carried out in collaboration with researchers at Imperial College in London who used a quartz reactor at atmospheric pressure [3]. Their results are shown in Fig. 2. Carbon selectivity to C_{2+} hydrocarbon products is plotted as a function of methane conversion. Selectivities of 30–50% are achieved at high methane conversions of 65–90%. The remainder of the converted methane forms mostly carbon monoxide in nearly a 1:2 molar ratio with hydrogen, making it a valuable synthesis gas for downstream upgrading. Fig. 2 also shows the Rule of “100” for oxidative coupling. This rule is based on the laboratory observation that the sum of C_{2+} selectivity and methane conversion for the best oxidative coupling catalysts does not exceed 100. All the BP oxidative pyrolysis results exceed the “100” Rule and do so at a very high methane conversion. This reduces,

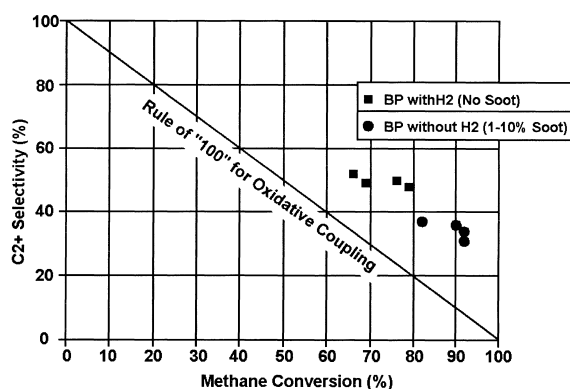


Fig. 2. British Petroleum oxidative pyrolysis results (US Patent 4 726 913).

and may eliminate all together, the need for expensive recycle of unconverted methane which is required in oxidative coupling. BP further reports that hydrogen coaddition with the methane and oxygen feed eliminates soot formation.

There are several attractive features of a spouted-bed oxidative pyrolysis process: (i) high per pass conversion of methane; (ii) valuable product mixture of syngas and C_2 hydrocarbons (mostly ethylene and acetylene); (iii) spouted-bed reactor offers excellent heat management providing a self-sustaining temperature upon ignition without external heat transfer; and (iv) reaction is accomplished thermally without a catalyst.

The results reported in this paper are based on a program undertaken at Amoco to evaluate the potential of oxidative pyrolysis in a spouted-bed reactor for natural gas conversion. The intent was to: (i) experimentally verify yield reported in the BP patents; (ii) establish the feasibility of operating at higher pressures (8–35 atm); and (iii) evaluate ways to increase C_{2+} product yield, such as by hydrogen coaddition, rapid thermal quench, and optimization of process conditions.

2. Reaction stoichiometry

Detailed product analyses from two of the BP experiments are given in Table 1: one without hydrogen coaddition (experiment 1 with a methane to oxygen feed ratio 1:6:1) and the other with hydrogen

Table 1
British Petroleum methane oxidative pyrolysis results in a spouted-bed reactor (US Patent 4726913)

Bed material	Expt. no. 1 crushed firebrick	Expt. no. 7 quartz chips
CH ₄ /O ₂ feed ratio	1.64	1.63
H ₂ /O ₂ feed ratio	0	1.63
GHSV	17.700	20.800
CH ₄ conv. (%)	82	79
C ₂₊ yield (%)	30	38
<i>Product distribution (vol%)</i>		
CH ₄	7.0	6.5
N ₂	3.0	2.8
H ₂	32.9	47.6
CO	15.4	11.5
CO ₂	2.0	1.2
H ₂ O ^a	34.0	24.7
C ₂ H ₂	3.9	3.4
C ₂ H ₄	1.5	2.1
C ₂ H ₆	0	Trace
C ₆ H ₆	0.3	0.2
Carbon make (carbon selectivity) (%) ^b	20	0

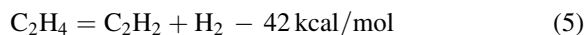
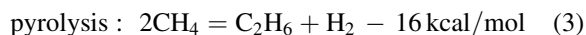
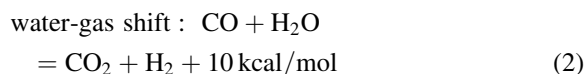
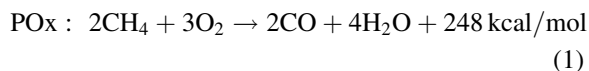
^aCalculated from oxygen material balance.

^bCalculated from carbon material balance.

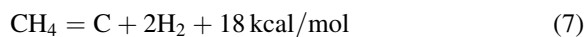
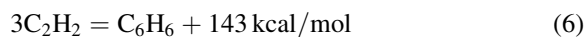
coaddition (experiment 7 with a methane to oxygen feed ratio of 1:1.6:1). The results were reported on a moisture and carbon free basis, so water was back calculated from an oxygen mole balance and solid

carbon (soot) was back calculated from a carbon mole balance. With hydrogen coaddition, the material balance in Table 1 reveals that there was soot made which is consistent with BP's experimental observations.

These oxidative pyrolysis results are consistent with a simple reaction network which combines partial oxidation and pyrolysis reactions:



Cyclization/carbon formation:



With a stoichiometric methane to oxygen feed ratio of 1.6:1, about half of the methane is consumed by reaction (1) (oxidation) and the remainder by mostly reaction (2) (pyrolysis). Other than the partial oxidation reaction, the other steps are severely constrained by thermodynamic equilibrium. Fig. 3 plots the loga-

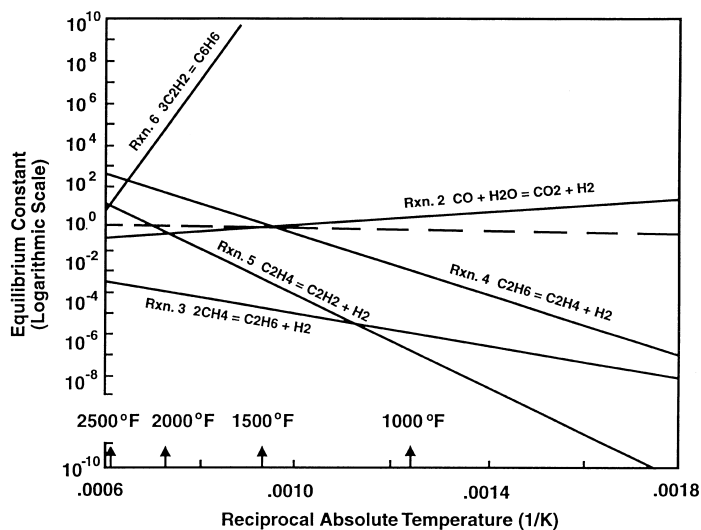


Fig. 3. Thermodynamic equilibrium constants for oxidative pyrolysis reactions.

Table 2

Comparison of BP oxidative pyrolysis experimental results with thermodynamic equilibrium

Reaction	Product ratio (mole fraction)	Calc. equil. temp. (°F)	Adiabatic reaction temp. (°F)
<i>BP expt. no. 1 (see Table 1)</i>			
(2) $\text{CO} + \text{H}_2\text{O} = \text{CO}_2 + \text{H}_2$	$(\text{CO})(\text{H}_2)/(\text{CO}_2)(\text{H}_2\text{O})$	4470	2370
(3) $2\text{CH}_4 = \text{C}_2\text{H}_6 + \text{H}_2$	$(\text{C}_2\text{H}_6)(\text{H}_2)/(\text{CH}_4)^2$	–	
(4) $\text{C}_2\text{H}_6 = \text{C}_2\text{H}_4 + \text{H}_2$	$(\text{C}_2\text{H}_4)(\text{H}_2)/(\text{C}_2\text{H}_6)$	2350	
(5) $\text{C}_2\text{H}_4 = \text{C}_2\text{H}_2 + \text{H}_2$	$(\text{C}_2\text{H}_2)(\text{H}_2)/(\text{C}_2\text{H}_4)$	1990	
(6) $3\text{C}_2\text{H}_2 = \text{C}_6\text{H}_6$	$(\text{C}_6\text{H}_6)/(\text{C}_2\text{H}_2)^3$	2350	
(7) $\text{CH}_4 = \text{C} + 2\text{H}_2$	$(\text{H}_2)^2/(\text{CH}_4)$	1080	
<i>BP expt. no. 7 (see Table 1)</i>			
(2) $\text{CO} + \text{H}_2\text{O} = \text{CO}_2 + \text{H}_2$	$(\text{CO}_2)(\text{H}_2)/(\text{CO})(\text{H}_2\text{O})$	3270	2300
(3) $2\text{CH}_4 = \text{C}_2\text{H}_6 + \text{H}_2$	$(\text{C}_2\text{H}_6)(\text{H}_2)/(\text{CH}_4)^2$	–	
(4) $\text{C}_2\text{H}_6 = \text{C}_2\text{H}_4 + \text{H}_2$	$(\text{C}_2\text{H}_4)(\text{H}_2)/(\text{C}_2\text{H}_6)$	2570	
(5) $\text{C}_2\text{H}_4 = \text{C}_2\text{H}_2 + \text{H}_2$	$(\text{C}_2\text{H}_2)(\text{H}_2)/(\text{C}_2\text{H}_4)$	1980	
(6) $3\text{C}_2\text{H}_2 = \text{C}_6\text{H}_6$	$(\text{C}_6\text{H}_6)/(\text{C}_2\text{H}_2)^3$	2350	
(7) $\text{CH}_4 = \text{C} + 2\text{H}_2$	$(\text{H}_2)^2/(\text{CH}_4)$	1180	

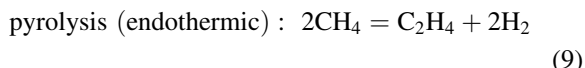
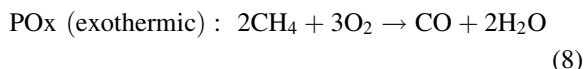
rithm of the equilibrium constant as a function of reciprocal temperature for reactions (2)–(6). For significant methane conversion by pyrolysis, the combination of reactions (3) and (4) require temperatures greater than 1000°C.

From the experimental results in Table 1, the equilibrium temperatures for the reported product ratios were calculated with the help of Fig. 3. The results are given in Table 2. The predicted equilibrium temperatures are very close to one another and within the temperature range for the oxidative pyrolysis experiments of 1100–1300°C.

Oxidative pyrolysis is an elegant mixture of partial oxidation and pyrolysis reaction. Pyrolysis provides high methane conversion to ethylene/acetylene and coproduces hydrogen. Partial oxidation provides thermal heat, minimizes coke, and produces carbon monoxide. Hydrogen and carbon monoxide are synthesized at a ratio of about 2:1, making it an excellent synthesis gas for upgrading. More than enough heat is produced by oxidation to meet the demands of the endothermic pyrolysis reactions. At adiabatic conditions, enough heat is left over to conveniently preheat the feed to reaction conditions of 1000–1300°C. Thus, the overall system becomes self-sustaining without any need for external heat addition/removal upon start-up. This type of process is termed adiabatic, autothermal operation.

For the purposes of understanding the distribution of oxidative pyrolysis gaseous products, reactions

(1)–(7) can be further simplified to three reactions:



This provides a starting point for understanding the oxidative pyrolysis reaction. If all the oxygen is consumed by reaction (8) and reactions (9) and (10) are at thermodynamic equilibrium, then there exists a single operating point at a given feed composition which represents the simultaneous solution of the adiabatic heat balance and the material balance which is constrained by thermodynamic equilibrium.

The BP experiments reported in [2] were conducted at the following two feed compositions: methane to oxygen: 1.6:1 and methane to hydrogen to oxygen 1.6:1.6:1. For these two feed ratios, the observed performance (adiabatic temperature, methane conversion, and C_2 selectivity) is compared with that predicted by reactions (8)–(10). Whereas BP did not report their reaction temperatures, the predicted methane conversion of 91% compares well with the observed range 82–92% for a 1.6 methane to oxygen feed, but the predicted C_2 yield is about 20% (absolute) higher than reported. It is believed that this difference is probably due to coke formation which is not accounted for by the simple stoichiometry of

Table 3

Comparison of BP oxidative pyrolysis results with those evaluated from proposed reaction network (reactions (1)–(7))

Product distribution (vol%)	Expt. no. 1		Expt. no. 7	
	BP	Calc.	BP	Calc.
CH ₄	7.0	6.6	6.5	6.3
N ₂	3.0	3.0	2.8	2.8
H ₂	32.9	33.4	47.6	48.3
CO	15.4	15.8	11.5	11.5
CO ₂	2.0	2.0	1.2	1.2
H ₂ O	34.0	33.6	24.7	24.3
C ₂ H ₂	3.9	3.9	3.4	3.3
C ₂ H ₄	1.5	1.5	2.1	2.0
C ₂ H ₆	0	0	0.04	0.04
C ₆ H ₆	0.3	0.3	0.2	0.2

reactions (8)–(10). Without coke formation, Table 3 shows that experimental and predicted results are in excellent agreement.

The simple stoichiometry of reaction (8)–(10) also provides a basis for optimization. With this approach, Fig. 4 shows the predicted C₂ yield (methane conversion multiplied by selectivity to C₂ products) at a constant methane to hydrogen feed ratio fixed at 1:1. There is a theoretical optimum of 40–45% in C₂ yield at a methane to oxygen feed ratio of about 1.3:1. To the

Table 4

Thermodynamic allowability for graphitic carbon formation at CH₄/O₂ feed ratio of 1.6

Temperature (°F)	H ₂ /O ₂ feed ratio					
	0	1.0	1.3	1.6	2.0	3.2
2730	NC ^a	NC	NC	NC	NC	NC
2280	NC	NC	NC	NC	NC	NC
1830	NC	NC	NC	NC	NC	NC
1650	NC	NC	NC	NC	NC	NC
1470	NC	NC	NC	NC	NC	NC
1290	C ^b	NC	NC	NC	NC	NC
1110	C	C	C	C	C	NC
930	C	C	C	C	C	NC
750	C	C	C	NC	NC	NC
570	C	C	NC	NC	NC	NC
390	C	C	NC	NC	NC	NC

^aNC=carbon formation not allowed at thermodynamic equilibrium.

^bC=carbon formation allowed.

left of the maximum (oxygen rich), selectivity dominates the C₂ yield term as too much carbon monoxide is being produced by partial oxidation. To the right of the maximum (oxygen lean), conversion dominates the C₂ yield term as not enough heat is generated from insufficient partial oxidation to drive the equilibrium-limited pyrolysis reaction. Fig. 4 suggests that optimization of the methane to oxygen feed ratio could increase C₂ yield over that reported by BP.

BP reported that hydrogen coaddition prevents sooting. Indeed, preliminary experiments at Amoco confirm that the sand remains white (clean) with hydrogen coaddition but is completely blackened without hydrogen. With reaction (1)–(7), coke (graphitic carbon) formation was analyzed by a thermodynamic equilibrium viewpoint. The results are given in Table 4 at a constant methane to oxygen feed ratio of 1.6:1 while varying the hydrogen to oxygen ratio from 0:1 to 3.2:1. Whereas coking is not eliminated at BP conditions at a hydrogen to oxygen feed ratio of 1.6:1, its window for formation is significantly narrowed. Of course, this does not address soot formation which would occur by free radical polymerization. Vinyl radicals (C₂H₃) formed in the pyrolysis process are known coke precursors. Hydrogen may either quench these radicals kinetically or reduce their concentration because of thermodynamic equilibrium limitations. Another way to thermally quench products and prevent coking may be with steam addition.

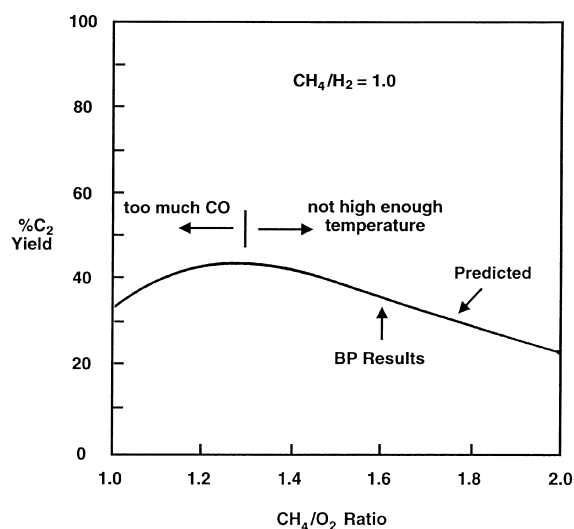


Fig. 4. Theoretical C₂ yield for methane oxidative pyrolysis based on adiabatic equilibrium results (reactions (8)–(10)).

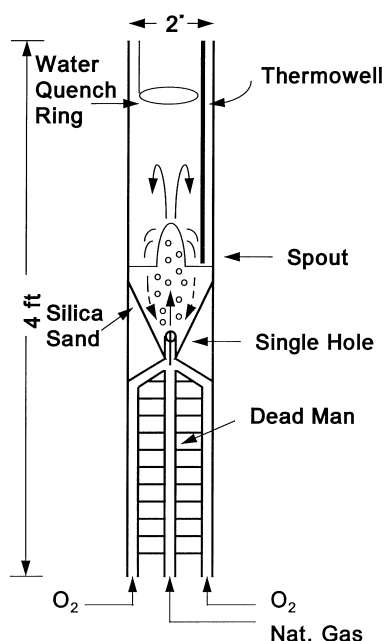


Fig. 5. Experimental spouted-bed reactor.

3. Experimental reactor design modifications

Reacting pure oxygen and methane at temperatures greater than 1100°C and high pressures is a complicated task. An integrated reactor system was designed that satisfies safety and material requirements. The spouted-bed tube measures 5 cm ID by 122 cm long (see Fig. 5). The spouted-bed reactor with conical distributor is sealed inside a Hastelloy tube with an outer shell. This system is made leak tight with an O-ring gasket which allows easy removal of the spouted-bed tube. Under reaction conditions, a slightly higher pressure is maintained on the outside walls of the spouted-bed tube. This procedure keeps the tube under compression for greater strength. Fig. 6 shows the reactor shell into which the spouted-bed reactor is inserted. External thermocouples and inlet and outlet furnaces are attached to the Hastelloy tube inside the reactor shell. The inlet furnace is used for start-up to preheat the feed to a high enough temperature for self-ignition. The outlet furnace is used to make up heat losses which permits adiabatic conditions to be reached.

An existing pilot plant was modified to accommodate the reactor shell in a containment cell, which

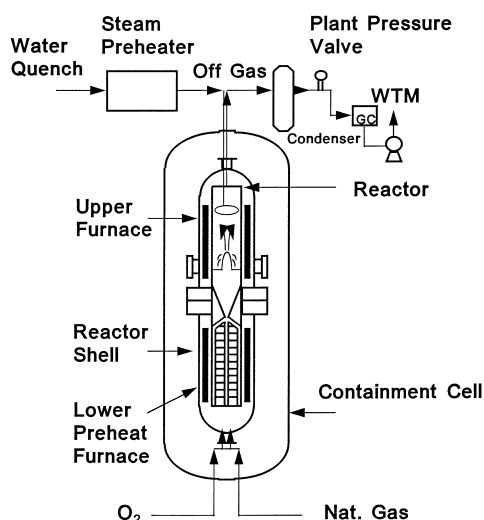


Fig. 6. Simplified process flowsheet for oxidative pyrolysis reactor.

provides additional safety shielding. Fig. 6 shows a simplified flowsheet of modified pilot plant to accept the spouted-bed reactor. This involved: (i) repiping the downstream tubing to minimize pressure drop; (ii) adding a water quench system for the spouted-bed reactor (see Fig. 5 which shows the quench ring inside the reactor); (iii) installing an on-line HP5880 gas chromatograph with TCD/FD detectors for complete product and feed analysis; and (iv) adding a high flow, heated filter assembly consisting of eight 1 ft long filter elements to capture any product tars and prevent downstream plugging.

Cold flow studies were conducted to establish critical properties for designing a spouted-bed reactor with silica sand as heat carrier, which include gas flow rate, reactor entrance tube diameter (1/16 in.), cone angle (20°, same as in BP design), reactor diameter (5 cm, same as in BP design), particle size (35 mm), particle density (1.7 g/cc density), and particle type for attrition resistance (silica sand). While it is recognized that interest may exist in testing other heat carriers, silica sand was selected because of its low cost and good attrition properties. Fig. 7 shows a flow regime map for the 5 cm diameter spouted-bed reactor. The gas velocities for acceptable spouting fall within a narrow band, which constrains the range of space velocities for process variable studies.

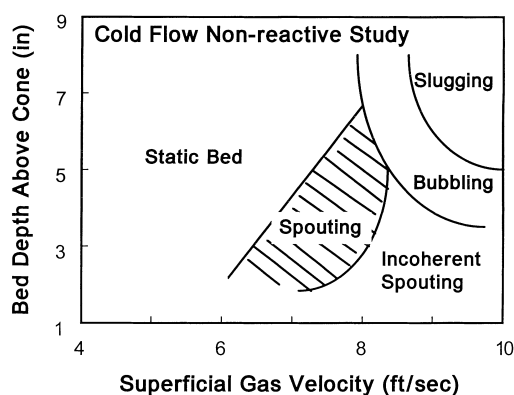


Fig. 7. Flow regime map for stable spouting in experimental spouted-bed reactor for silica sand.

Fig. 5 shows details of the spouted-bed reactor. At the inlet, natural gas flows into the annulus of a deadman and oxygen flows on the outside. The two mix at the bottom of the conical spouted bed. Initial experiments showed that the silica sand was maintained in the reactor, high operating temperatures of 1100°C were achievable, and feed preheat/ignition system worked satisfactorily. Originally, the reactor tube was fabricated from quartz. Quartz is a brittle material that must be kept under compression. The design of the reactor shell/tube allowed for this, and indeed the quartz tube did not break at the outer walls. However, the stresses at the spouted bed cone are not perpendicular because of its complex shape. This leads to breakage problems that could not be solved in spite of many design changes to strengthen this

area. Moreover, inherent tolerances in quartz manufacture of wall thickness, roundness, and straightness likely contributed to stresses that caused the quartz to fracture. Consequently, we switched from a quartz reactor to one made of 310 Stainless Steel. As seen in Table 5, the stainless steel reactor produces about three times more carbon dioxide compared with carbon monoxide (about 1:3 carbon dioxide to carbon monoxide) than the quartz reactor (about 1:10 carbon dioxide to carbon monoxide). The stainless steel walls catalyze the deep oxidation of methane to carbon dioxide and water. To minimize this effect, the stainless steel tube was alonized which involves coating the walls with an aluminum oxide layer. As seen in Table 5, this modification reduces the amount of carbon dioxide back to the level reported by British Petroleum for their quartz reactor. There is a concern that the alonized layer may not be stable at reaction temperatures greater than 1100°C. We are searching for alternative coatings.

4. Preliminary experimental results

There have been a number of runs stopped because of high pressure drop and broken quartz tubes. Nevertheless, some preliminary findings have been obtained. One experimental run with the alonized stainless steel reactor tube is given in Table 6. Material balances for carbon, hydrogen, and carbon give tight closures. The highest conversion is 65% at a 30% selectivity to C₂₊ products, giving a C₂₊ yield of 19%.

Table 5

Oxidative pyrolysis results for different materials of construction for spouted-bed reactor (feed ratios: CH₄/O₂=1.6, H₂/O₂=1.6)

Product distribution (vol%)	Quartz reactor (BP expt. no. 7 from Table 1)	Stainless steel reactor (AOC expt. 15819-118-3)	Stainless steel coated with alumina (AOC expt. 15819-124-3)
CH ₄	6.5	18.3	11.2
N ₂	2.8	0.7	7.7
H ₂	47.6	31.0	34.2
CO	11.5	11.5	13.9
CO ₂	1.2	4.3	1.6
H ₂ O	24.7	32.6	28.2
C ₂ H ₂	3.4	0.3	0.5
C ₂ H ₄	2.1	1.0	1.8
C ₂ H ₆	Trace	0.1	0.2
C ₆ H ₆	0.2	0.02	0.2
CO/CO ₂ product ratio	9.6	2.7	8.7

Table 6

Oxidative pyrolysis preliminary experimental results in alonized-stainless steel spouted-bed reactor with silica sand

	Expt. 19819-124		
	No. 2	No. 3	No. 4
Reaction temp. (°F)	1880	1880	1880
CH ₄ /O ₂ feed ratio	1.5	1.5	1.5
H ₂ /O ₂ feed ratio	1.3	1.3	1.3
N ₂ /O ₂ feed ratio	0.3	0.3	0.3
CH ₄ conv. (%)	63	64	65
C ₂₊ selectivity (%)	31	29	30
C ₂₊ yield (%)	19	19	19
<i>Product distributon (vol%)</i>			
CH ₄	11.0	11.2	10.9
N ₂	7.0	7.7	8.0
H ₂	36.3	34.2	34.0
CO	13.7	13.9	13.5
CO ₂	1.6	1.6	1.6
H ₂ O	27.5	28.2	29.0
C ₂ H ₂	0.5	0.5	0.5
C ₂ H ₄	1.8	1.8	1.8
C ₂ H ₆	0.2	0.2	0.2
C ₆ H ₆	0.2	0.2	0.2
<i>Material balance (product to feed ratio)</i>			
Hydrogen	0.98	0.96	0.94
Carbon	0.99	0.99	0.95
Oxygen	1.02	1.05	1.03
Nitrogen	1.00	1.00	1.01

Table 7 compares our preliminary results with those reported by BP at similar conditions. While our C₂₊ yields are lower than those of BP, they rival the best oxidative coupling catalysts giving a selectivity plus conversion of 95% (refer to the oxidative coupling Rule of “100” in Fig. 2). The reason for our C₂₊ yields being lower than expected can be understood by examining reactor temperature. The temperature of our run (measured by a quartz covered thermocouple) is less than the adiabatic temperature of 1260°C. This

Table 7

Comparison of British Petroleum and amoco results for spouted-bed oxidative pyrolysis

	BP range (US Patent 4 726 913)	Amoco expt. 15819-98-4	Amoco expt. 15819-124
CH ₄ /O ₂ feed ratio	1.6	1.6	1.6
H ₂ /O ₂ feed ratio	1.6	1.6	1.6
CH ₄ conv. (%)	66–79	50	65
C ₂₊ yield (%)	35–39	7	19
Reaction temp. (°F)	Not reported	1780	1880
Adiabatic temp. (°F)	2300	2300	2300

is caused by the high heat losses from our reactor. Experimentally, this will be corrected by heating the upper zone furnace to reach the adiabatic temperature. High temperatures are critical to obtain higher methane conversions and better C₂₊ selectivities because of the limitations imposed by thermodynamic equilibrium.

We have been unsuccessful so far in heating the tube to temperatures higher than 1100°C. The pressure drop across the inlet 1.6 mm spout orifice becomes unacceptably high because of coke plugging. We are working to solve this problem.

5. Conclusions

1. Stoichiometry suggests that oxidative pyrolysis is a simple combination of methane partial oxidation to carbon monoxide which provides heat to drive methane pyrolysis to ethylene and acetylene.
2. Methane pyrolysis is thermodynamically limited and requires temperatures in excess of 1100°C for reasonable conversion.
3. Stoichiometric analysis provides a modeling tool for understanding results and guiding experiments. For example, theoretical results suggest that the C₂₊ yield observed by BP may be increased 10–15% by lowering the methane to oxygen ratio.
4. Our experimental findings support those reported by British Petroleum that hydrogen addition significantly reduces coke formation. Thermodynamic equilibrium shows that the window for graphic coke formation is narrowed by hydrogen addition. Kinetic arguments that hydrogen quenches coke precursor radicals are also consistent with this result.
5. A spouted-bed reactor was designed from cold flow studies to verify the BP results and to establish process feasibility at higher pressures. It has

evolved from a fragile quartz tube to a more robust one of stainless steel. The stainless steel performs similarly to the quartz reactor when the walls are coated with an aluminum oxide layer to passivate inherent catalytic activity.

6. While scoping economic studies of an oxidative pyrolysis process are very attractive, the spouted-bed reactor system is complicated by safety and material requirements. In spite of these experimental challenges, preliminary runs have been successful in demonstrating several features: (i) preheating the feed ignites the reaction which becomes self-sustaining; (ii) detailed material balances give excellent closure; and (iii) high operating temperatures are achievable (at least up to 1100°C).

Acknowledgements

Tony LaPuma has played an integral part throughout this program in cold flow studies, equipment design, and unit operation.

References

- [1] Encyclopedia of chemical technology, Acetylene, vol. 1, 3rd ed., Wiley, New York, 1978.
- [2] US Patent 4 726 913.
- [3] F.J. Weinberg, T.G. Barlett, F.B. Carleton, P. Rimbotti, J.H. Brophy, R.P. Manning, *Combustion and Flame* 72 (1988) 235–239.